phys. stat. sol. (a) **174**, 25 (1999)

Subject classification: 68.55.Nq; 68.60.Wm; 78.66.Db; S5

Nitrogen Incorporation into Tetrahedral Hydrogenated Amorphous Carbon

S. E. Rodil, N. A. Morrison, J. Robertson, and W. I. Milne

Engineering Department, University of Cambridge, Cambridge CB2 1PZ, UK

(Received March 25, 1999)

Structural changes induced by the incorporation of nitrogen into ta-C:H films have been studied by Electron Energy Loss Spectroscopy, X-Ray Photoelectron Spectroscopy, Fourier Transformed Infrared Spectroscopy and Ultraviolet-Visible Spectroscopy. ta-C:H films have been synthesised using a low pressure Electron Cyclotron Wave Resonance (ECWR) source which provides a plasma beam with a high degree of ionisation and dissociation. Nitrogen was incorporated by adding N_2 to the C_2H_2 plasma used for the deposition of ta-C:H films. The N/C atomic ratio in the films rises rapidly until the N_2/C_2H_2 gas ratio reaches three, and then increases more gradually, while the deposition rate decreases steeply. Chemical sputtering of the forming films and the formation of molecular nitrogen within the films limit the maximum nitrogen content to about N/C = 0.6. For low nitrogen content the films retain their diamond-like properties, however as N/C atomic ratio increases, a polymeric-like material is formed, with >C=N− structures and terminating C≡N and NH groups that decrease the connectivity of the network.

1. Introduction

Amorphous hydrogenated carbon (a-C:H or DLC) films have an extensive range of applications, because of their unique properties, such as, hardness, low coefficient of friction, chemical inertness and infrared transparency [1]. These properties are determined by the C–C bonding configurations present, i.e., the fraction of sp^2 and sp^3 carbon atoms, and the hydrogen content in the films. The mechanical properties are controlled by the fraction of sp^3 bonded carbon, forming the skeleton of the material. The optical and electronic properties are determined by the clustering (ring or chains) of the sp^2 sites. Finally, the fraction of hydrogen decreases the connectivity of the sp^3 matrix by forming terminating CH groups, and therefore lowers the hardness of the films. The sp^3/sp^2 fraction and H content can be adjusted by varying the deposition parameters [2]. Conventional plasma deposition processes result in films where, both the H content and the sp^3 fraction decreases with increasing the ion energy, so that films are polymeric at low ion energy and graphitic at high ion energy. This has been attributed to the low plasma density and high deposition pressure of the systems [3].

Recently, the development of high density, low pressure plasma sources has led to the deposition of a highly tetrahedral (sp^3 fraction around 70%) form of a-C:H with low H content (<30%), named ta-C:H [4]. In this case the film growth is controlled by ion bombardment that promotes the formation of sp^3 C–C bonds and decreases the H content. The use of these films for specific technical applications has still to be investigated. For example, for electronic applications the doping efficiency has to be addressed, while their use as a protective coating depends upon the reduction of the in-

trinsic stress. The stress is inherent to DLC films and it arises as a side effect from the use of an ion beam deposition process to stabilise the sp^3 bonding, using the physical process called subplantation [5]. In order to investigate these possibilities, nitrogen has been incorporated into ta-C:H films.

The deposition of nitrogen containing amorphous carbon has received particular attention since the theoretical predictions of a metastable silicon-nitride-like phase, i.e., β-C_3N_4 [6]. According to these predictions, this phase could present insulating properties, hardness and thermal conductivity comparable to those of diamond. However, most attempts have yielded amorphous material with a nitrogen content lower than the expected one (N/C = 4/3) and a low fraction of sp^3 bonded carbon [7]. In only a few cases has evidence for the formation of small crystallites embedded in an amorphous phase been presented [8, 9].

In this paper, we report the results on the growth behaviour, chemical composition, bonding structure and optical properties of a-C:N:H films deposited by an ECWR source using N_2/C_2H_2 plasmas and parameters based on the preparation of ta-C:H, since this would promote the formation of sp^3 CN bonds.

2. Experimental

The electron cyclotron wave resonance (ECWR) plasma beam source comprises a single turn electrode, surrounded by two Helmholtz coils through which a static transverse magnetic field is applied. High plasma densities can be produced by a resonant mechanism established by the interaction between the static magnetic field and an inductively coupled rf-current applied to the single turn electrode. The ion energy is controlled by an electrostatic acceleration extraction system, thus permitting the independent control of the ion energy (through variation of the plasma potential) and the current density (by rf-power and pressure) [10, 11].

The a-C:N:H films were deposited using N_2 and C_2H_2 as the source gases and similar deposition parameters as those previously used in the preparation of ta-C:H [10]. The ion energy was fixed at 80 eV to help minimise chemical sputtering of the carbon film by impinging N ions. The pressure prior to deposition was always less than 5×10^{-6} mbar, and during deposition remained below 5×10^{-4} mbar, but small variations occur as the nitrogen to acetylene ratio was varied from 0 to 7 (the total flow varied between 10 and 30 sccm). A Faraday cup mounted in the substrate place was used to measure the ion energy and ion current densities. The measured current density varied between 0.35 and 0.2 mA/cm^2 as a function of the nitrogen partial pressure due to the higher ionisation energy of nitrogen (14.6 eV) compared to acetylene (11 eV). All the films were deposited at room temperature onto single crystal Si (100) and 7059 Corning glass substrates.

2.1 Characterisation

The thickness of the films, ranging from 40 to 85 nm, was measured by fixed wavelength ellipsometry. The latter was also used to determine the refractive index of the films grown on Si at 632.8 nm. The film composition and bonding were measured by X-Ray Photoelectron Spectroscopy (XPS), Electron Energy Loss Spectroscopy (EELS) and Rutherford Backscattering (RBS).

The XPS analyses were carried out with a Perkin Elmer 5500 spectrometer using the Al Kα line (1486.6 eV). The relative composition of the films (N/C atomic ratio) was calculated from the ratio between the total area of the XPS signal of N 1s and C 1s core levels, using the sensitivity factor of the instrument (0.42 and 0.25, respectively). This calculation was performed from signals measured without any argon etching of the film surface, in order to avoid preferential sputtering of N atoms compared to C atoms. XPS spectra were also recorded after sputtering the film surface with 4 kV argon ions.

EELS measurements were carried out in a vacuum generator HB501 scanning transmission electron microscope with a dedicated parallel EELS spectrometer. The films were prepared by removing the Si substrate with a $HF:HNO_3:H_2O$ (1 : 8 : 4) acid solution. Some films were removed from the substrate in seconds without noticeable damage, while the others were only obtained when the silicon substrates were completely etched (indicating a different bonding structure). The remaining film segments were put into distilled water and then transferred to electron microscope copper grids.

Optical absorption spectra were derived from transmission and reflection measurements in an ATI-Unicam UV2-200 UV-VIS spectrometer. The absorption was derived using an iterative method to calculate the refractive index and extinction coefficient over the 300 to 1100 nm wavelength range [12]. The nature of chemical bonding was also determined by using a vacuum FTIR spectrometer (BONEM DA-3) in the 400 to 4000 cm^{-1} range. A total of 300 scans were used to improve the low signal to noise ratio due to the thickness of the films.

3. Results

3.1 Growth and composition

The main effect of the addition of nitrogen is the reduction of the deposition rate as shown in Fig. 1. There are two factors that cause this reduction. First, there are fewer CH growth species in the plasma as nitrogen is added to the gas phase. Secondly, there is a chemical sputtering of the growing film by energetic nitrogen ionic species [13]. To determine the amount of etching, we first measured the etching rate of a previously deposited a-C : H film using a nitrogen plasma at different ion energies. The results are plotted as an insert in Fig. 1 showing that for 80 eV and a current density of 0.15 mA/cm^2 the etching rate attained a value of 1.5 Å/s, comparable to the deposition rates obtained for high N_2/C_2H_2 ratios. However, further investigations are necessary to determine the mechanism involved in the etching process and its dependence upon other factors.

Fig. 2 shows the N/C atomic ratio as a function of nitrogen to acetylene flow ratio, N_2/C_2H_2, obtained by the three different methods. The lower values obtained by XPS might be due to the enhancement of the carbon signal by contamination of the film surface. Even though the absolute values do not coincide the trend is similar. Indicating a rapid incorporation of nitrogen at N_2/C_2H_2 ratios below three, while at higher N_2/C_2H_2 ratios the N/C atomic ratio seems to saturate at a value of 0.6. The maximum value is well below the 1.33 expected for the theoretical C_3N_4. This saturation value represents one of the major difficulties in forming carbon nitride films. A similar trend could be found in the nitrogen content of samples deposited by other systems, such as PECVD [14], dual ion beam [15, 16] and reactive magnetron sputtering [17, 18]. The composition was uniform through the film thickness as seen by SIMS and XPS profile analysis.

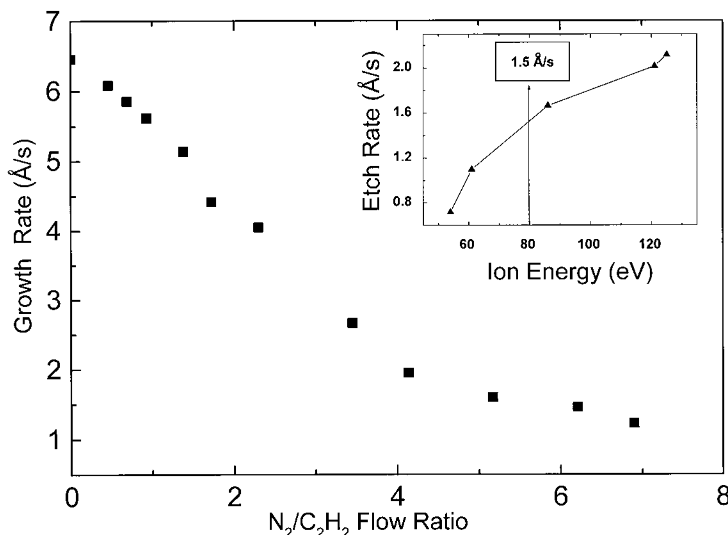

Fig. 1. Deposition rate as a function of the N_2/C_2H_2 flow ratio. The inset shows the etching rate of an a-C:H film deposited by conventional PECVD by a nitrogen plasma (ECWR source) at different ion energies

The explanation for the low nitrogen content is not only the chemical sputtering. It has been shown by TRIM calculations that a 65% nitrogen content could be attained in spite of the HCN and CN evolution [19]. Further investigations suggest that the formation of molecular nitrogen is responsible for the nitrogen evolution. Upon increasing nitrogen content in the films there is an increase in the probability of N–N bond formation, and thus the formation of molecular nitrogen, which can easily go into the gas phase [20, 21]. The formation of molecular nitrogen may be enhanced by ion bombard-

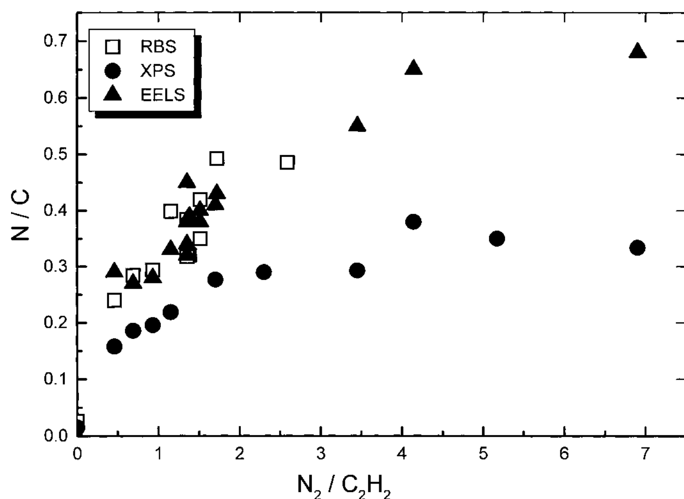

Fig. 2. Relative nitrogen concentration as a function of the N_2/C_2H_2 flow ratio as measured by three different methods. In the paper, N/C ratios of RBS or EELS will be used

ment through a knock on effect [22]. This N_2 can then diffuse to the surface or stay inside the film, inducing the formation of voids, which may account for the low density obtained in carbon nitride films. However, little evidence for the presence of N_2 bubbles has been found. In our case, this mechanism is supported by the fact that the nitrogen content was slightly higher for deposition at lower ion energies (40 eV) and by the presence of planar N–N bonds in the N 1s XPS results shown later.

3.2 Infrared

The IR spectra of some samples are shown in Fig. 3 for different N/C atomic ratios. In the spectrum obtained for the nitrogen-free sample (ta-C:H) the only feature is the C–H stretching band at 2900 to 3000 cm^{-1}. The nitrogen containing films show additional absorption bands: The N–H absorption band at 3300 to 3500 cm^{-1}, the C≡N stretching band at 2200 cm^{-1} and a broad band located around 1500 cm^{-1}. The latter is associated with different vibrational modes, including C–N (1250 to 1020 cm^{-1}), C=N imino groups (1610 to 1660 cm^{-1}), NH_2 bending (1590 to 1640 cm^{-1}), CH_x bending (1350 to 1450 cm^{-1}) and C=C bonds (1300–1500 cm^{-1}). In this region also the Raman active modes G (graphitic) and D (disorder) could become IR active due to the symmetrical breaking of the E_{2g} mode by nitrogen substitution of a few carbon atoms in graphitc microdomains [23].

When the N/C composition ratio is increased the following features becomes clear:

1. The absorption in the 1500 cm^{-1} region increases and becomes asymmetric with a clear maximum around 1600 cm^{-1}, characteristic of CN double bonds and NH modes.

2. The C≡N absorption increases, but is always low compared to its amount in the IR spectra of samples deposited by other methods [9]. No calculations have been made of the IR sensitivity for the CN triple bond, but through comparison with nitrogen containing polymers it is clear that the sensitivity strongly depends on the local environment.

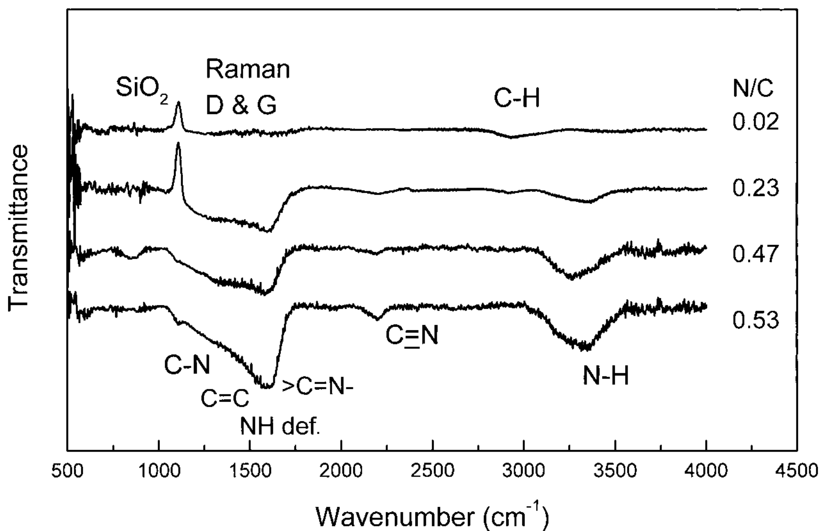

Fig. 3. Normalised transmission FTIR spectra taken from films with increasing nitrogen content. The main features are indicated in the figure. (The transmittance is given in arbitrary units)

3. Finally, the absorption of the CH_x stretching bands decreases, while the absorption of the NH band increases, indicating that hydrogen is preferentially bonded to nitrogen.

Similar trends have been reported [24], and it can be concluded that nitrogen incorporation leads to a polymeric structure with the formation of CN double bonds and hydrogen predominantly bonded to nitrogen.

3.3 XPS

For a detailed analysis the XPS core level lines were fitted by a convolution of a Gaussian and a Lorentzian profile and the background was subtracted using a Shirley type curve. The O1s was a sharp peak and it was fitted with one Gaussian at 533 eV to correct the spectra for any charging effect (not observed during the measurements), C 1s peak was not used as the influence of nitrogen was not certain. Fig. 4 shows the N 1s and C 1s core level of a-C:N:H samples with increasing nitrogen content.

The effect of nitrogen incorporation in the C 1s peak is an asymmetric broadening towards higher binding energy. For the non-nitrogenated film the C 1s peak is very sharp (FWHM = 1.48 eV) and is located at 285.4 eV, slightly higher than the value of other pure carbon hydrogen systems. As nitrogen is incorporated more components are necessary to fit the spectra, indicating that carbon is at least in four different binding states, including one peak for CO bonds. Even though some authors relate the different carbon configuration to sp^2 or sp^3 CN bonds [16], there is no evidence for a significant difference in the C 1s positions between graphite and diamond. Covalently it is more likely that the different binding energies correspond to a difference in the number of

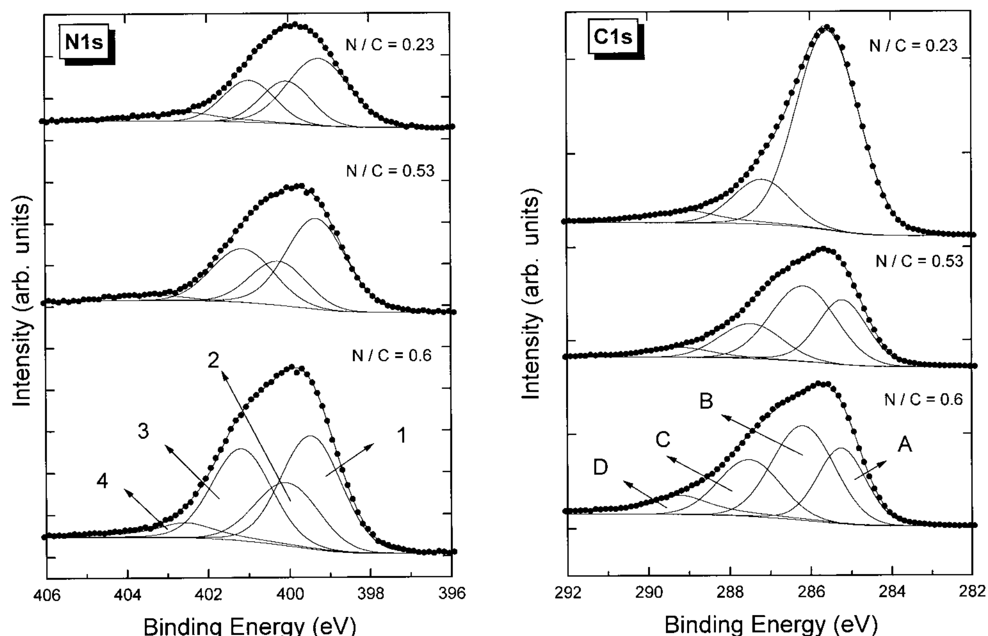

Fig. 4. XPS ($h\nu = 1486.6$ eV) core-level spectra of a-C:N:H samples prepared by ECWR as a function of N/C composition ratio. Dots are the measured data and lines represent fits as described in the text

Table 1

Fitting results from the analysis of the measured core-level lines. Four peaks were used in most cases and they are labelled A to D for C 1s and 1 to 4 for N 1s. During the fitting procedure all the parameters were left free adjustable, but a maximum value for the width of 1.8 eV was imposed. The line widths were between 1.4 and 1.8 eV

		C 1s				N 1s			
N_2/C_2H_2	N/C	peak A	peak B	peak C	peak D	peak 1	peak 2	peak 3	peak 4
		C–C	C–N_1	C–N_2	C–O	N–sp^3C	N–H	N–sp^2C	N–O, N–N
0.46	0.23	285.6	287.2		289.0	399.2	400.0	401.0	402.5
0.69	0.29	285.6	286.7	287.7	289.3	399.4	400.2	401.0	403.1
0.93	0.35	285.4	286.5	287.8	289.7	399.3	400.0	400.9	402.6
1.15	0.39	285.1	286.1	287.4	288.9	399.1	399.9	400.8	402.2
1.72	0.47	285.3	286.3	287.6	289.5	399.2	400.0	401.0	402.9
2.3	0.53	285.2	286.2	287.5	289.2	399.3	400.3	401.1	403.4
3.45	0.55	285.3	286.5	287.8	289.5	398.96	400.2	401.2	403.2
4.14	0.62	285.2	286.0	287.4	288.8	399.4	400.2	401.1	402.3
6.9	0.68	285.2	286.2	287.5	289.2	399.5	400.1	401.2	402.7

nitrogen neighbours [25], as shown in the assignments outlined in Table 1. The N 1s peaks are deconvoluted into four components. Peak 4 at higher binding energy can be assigned to NO, as oxygen was detected as a surface contaminant and may also result from N_2 molecules trapped in the film; this possibility will be discussed later. Peak 2 at 400 eV is assigned to both NH bonds [26] and CN triple bonds [27]. It has been confirmed that the presence of hydrogen introduces a component in a position intermediate between peaks 1 and 3, that are usually well resolved for non-hydrogenated CN films [26]. On the other hand, the assignment of peaks 1 and 3 is controversial, mainly because CN polymers and organic molecules are used as reference materials, which are poor conductors and no reliable binding energies have been assigned. In this paper, we assign the peak at lower binding energy (peak 1: 399 eV) to nitrogen bonded to sp^3 C and the peak at higher binding energy (peak 2: 401 eV) to nitrogen bonded to sp^2 C following the comparison of the N 1s peak position with reference data from nitrogen containing polymers and organic molecules [27, 28]. However, this contradicts the data obtained from pyromethene which contains N and C atoms, but no sp^3 carbon [29, 30]. Nevertheless, Souto et al. [31] recently compared the valence and core level electronic structures of sputtered a-CN_x films with a theoretically calculated density of states and core level binding energies of molecules containing sp^2/sp^3 CN bonds. The combined analyses of core level and valence band spectra lead to the conclusion that the peak at lower energy is related to N atoms in configurations with isolated lone pairs (including threefold-coordinated N atoms bonded to sp^3 C), while the peak at higher binding energy corresponds to substitution of N in graphite-like configurations, where the lone pairs are involved in stronger π bonds (this includes N atoms bonded to sp^2 C). This latter interpretation by Souto is more general and may be a clue for the interpretation of the XPS spectra in carbon nitrides.

The relative areas of the core level peak components are shown in Fig. 5. It can be seen that nitrogen is initially bonded to fourfold-coordinated carbon atoms, as expected for a ta-C:H sample where at least 60% of the carbon atoms are sp^3 hybridised. However, this picture is reversed for N/C composition ratios above 0.4, where nitrogen is preferentially bonded to threefold coordinated carbon atoms. The number of C–C

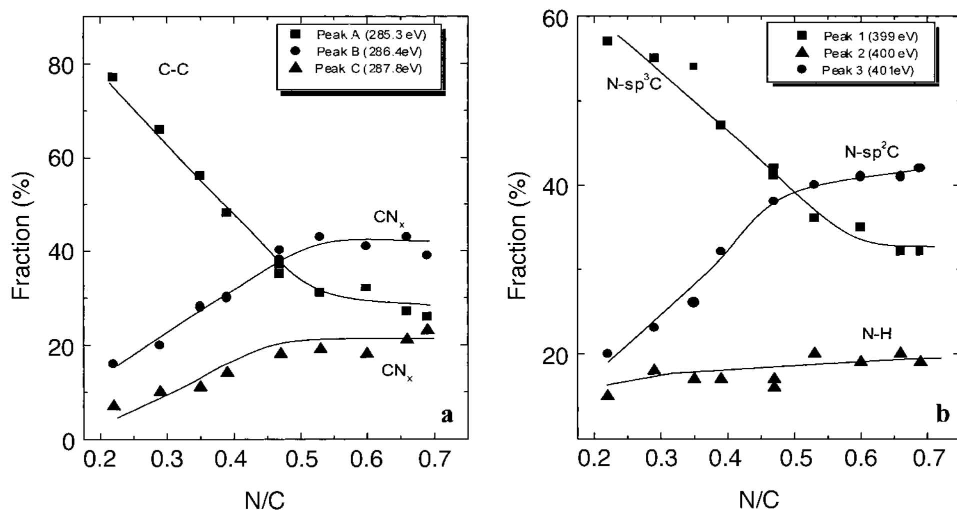

Fig. 5. Fraction of the components to the a) C 1s and b) N 1s core level spectra as outlined in Table 1

bonds is reduced as nitrogen is incorporated while the level of CN_x bonding gradually rises. There is no evident trend in the shift of either N 1s or C 1s peaks.

The presence of trapped molecular nitrogen in CN films deposited at low energies is of importance, since it may demonstrate that the key process responsible for the saturation of the nitrogen content within the films is the formation of molecular nitrogen either at or below the film surface. After *in situ* sputtering of the films, analysis of the

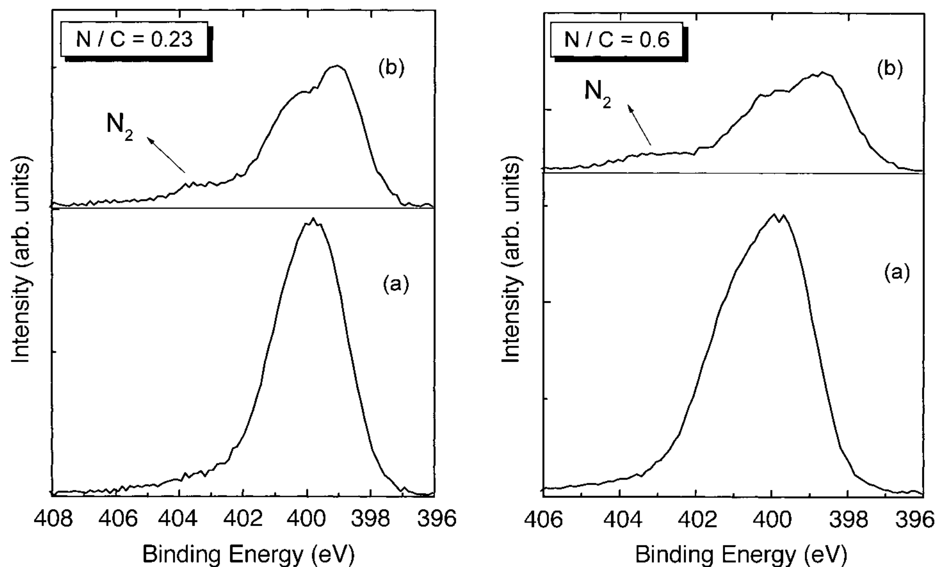

Fig. 6. XPS spectra of the N 1s level obtained a) prior and b) after Ar sputtering for two CN samples at different N/C composition ratios as shown in the figure

N 1s core level spectra showed a strong reduction of the nitrogen content and some structural changes induced by the bombardment as seen by other groups [25]. The two main components were well resolved, suggesting the evolution of hydrogen as a consequence of the bombardment (Fig. 6). However, the most interesting feature is that peak 4 at 402 eV remains after the sputtering process. As oxygen has already been removed, this peak may now be undoubtedly assigned to the presence of N–N planar bonds. The high intensity also suggests that molecular N_2 is present within the film. The presence of trapped N_2 in CN films has previously been reported by Grigull et al. [29], where N was implanted (20 keV) in hard amorphous carbon films at both room temperature (RT) and high temperature (HT). They demonstrated that during room temperature implantation, molecular nitrogen was formed within the films.

3.4 EELS

Electron energy loss spectroscopy can be used to determine the N/C atomic ratios and the nature of the carbon and nitrogen bonding. The high-loss spectrum consists of absorption edges from each element's core level and the absorption above the edge is proportional to the local density of conduction states surrounding the atoms. The C K-edge consists of a step at 290 eV due to transition from the C 1s core level to σ^* states and a peak at 285 eV due to transitions to π^* states of sp^2 and sp^1 states. The N K-edge spectrum is similar to that of carbon, the 1s– π^* and 1s–σ^* transitions are at energies 399 and 407 eV, respectively. Assuming that carbon is only present in sp^2 and sp^3 hybridisation, the fraction of sp^2 bonded carbon can be calculated by using the normalised area under the 1s–π^* peak, which is then compared with that of a 100% sp^2 bonded amorphous carbon standard [32].

In the samples with low nitrogen content, the C 1s–π^* transition appears as a shoulder on the 1s–σ^* peak, but this shoulder increases with increasing nitrogen content to form a clear peak. On the other hand, the N 1s–π^* peaks are well defined in all the samples independently of the nitrogen content, suggesting that nitrogen is bonded in the sp^2 hybridisation state. However, it is not possible to distinguish between planar-triangular or linear sp^2 structures from this data.

The evolution of the sp^2 carbon fraction is shown in Fig. 7. For low nitrogen content the sp^2 fraction is still low. As the nitrogen content increases, there is an increase in the

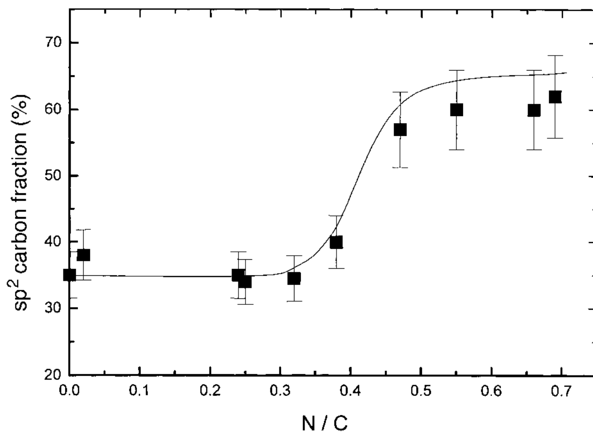

Fig. 7. The percentage of sp^2 bonded carbon as a function of nitrogen content

sp^2 fraction. This is a consequence of the reduction of the sp^3 CH bonds within the amorphous network and the formation of CN double bonded structures. The sp^3 content obtained by EELS in the a-C:N:H networks is the result of sp^3 C–C plus sp^3 C–H and sp^3 C–N bonds. The retention of the diamond-like properties of the films at low N/C ratios infers that the C–C single bonds are in fact substituted by C–N single bonds. Wan and Egerton [33] and Grigull et al. [29] found a fraction of sp^2 bonded carbon higher than 100% for carbon nitride samples deposited by carbon arc evaporation in N_2 or NH_3 atmosphere and ion beam assisted filtered cathodic vacuum arc, respectively. They explained their results by the high concentration of sp^1 carbon in their samples. In our case, the fraction of sp^2 bonded carbon is always much lower than 100%, so the sp^1 bonds, even though they may be present (as shown by the IR spectra) can be neglected.

From the low-loss region of the spectra, the plasmon valence energy can be calculated. Since it is proportional to the square root of the electron density, the plasmon energy is a rough measure of film mass density [34]. For a ta-C:H film with 30% H and a mass density of about 2.4 g/cm^3 (measured also by X-ray reflectivity) [35], the plasmon energy is 28.4 eV. With increasing N concentration the plasmon energy decreases to 24 eV. This implies a reduction in electron density when compared with ta-C:H and as N has one valence electron more than C, it also indicates a strong decrease in mass density.

3.5 Optical properties

The variation of the real (n) and imaginary (k) components of the refractive index as a function of the energy for different nitrogen contents can be seen in Fig. 8. The dispersion of n and k is similar for nitrogenated and non-nitrogenated samples. The films with the higher N percentage are slightly more absorbing at lower energy compared to a ta-C:H sample, however, the values are still low, confirming the non-graphitic structure.

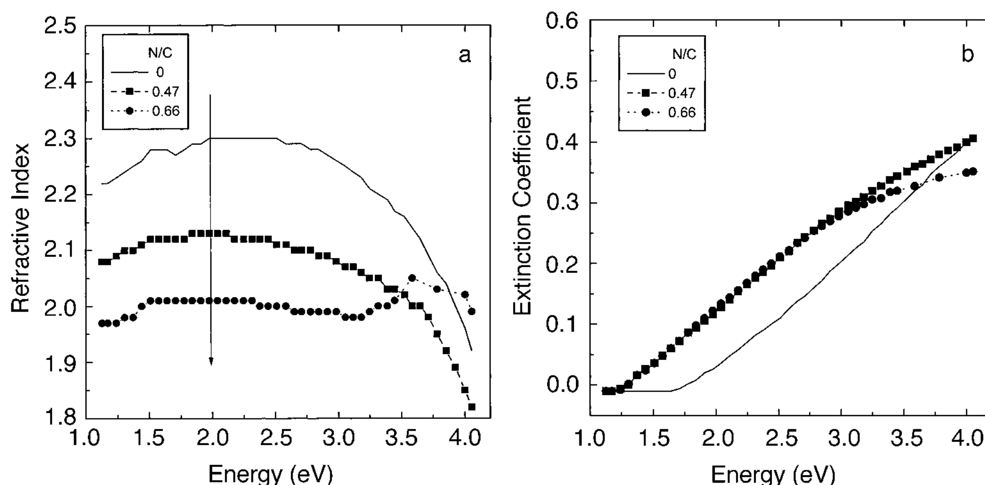

Fig. 8. Optical dispersion relations for N/C composition ratios, a) refractive index, b) extinction coefficients

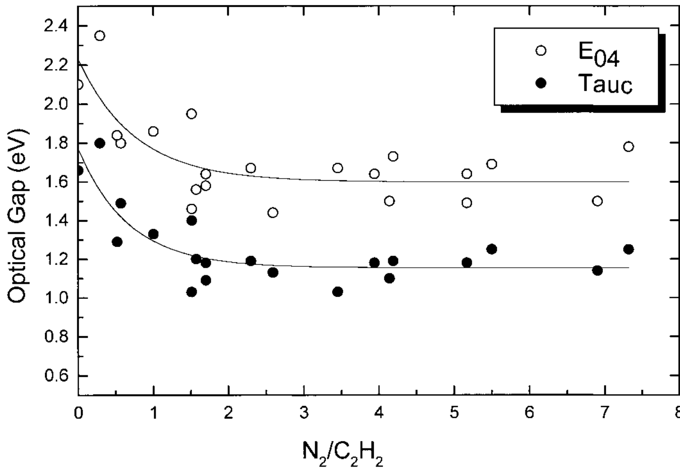

Fig. 9. Variation in the optical gap as a function of the N_2/C_2H_2 flow ratio

The refractive index decreases from 2.3 for ta-C:H to 2.0 for the more nitrogenated sample.

The Tauc and the E_{04} gap can both be calculated from the absorption spectra and they are presented as a function of nitrogen to acetylene ratio in Fig. 9. The optical gap decreases rapidly for low nitrogen incorporation and remains stable for a N/C composition ratio above 0.4. It is widely known that the band gap in all forms of amorphous carbon is primarily determined by the sp^2 fraction, so the decrease of the Tauc gap from 1.4 to about 1.1 eV can be explained by the increase in the sp^2 C fraction determined by EELS. However, the first decrease of the gap in the intermediate N/C region between 0.1 and 0.4, where the sp^2 fraction remains almost constant could be attributed to the appearance of the N lone pair electrons, as they lie in the top of the valence band.

4. Discussion

The findings of an increase of the sp^2 C fraction, decrease in mass density, increase in intensity of a band associated with polymeric CN structures in the IR spectra and strong changes of the components in the N 1s spectra indicate a modification of the structure on N incorporation.

From these results we can conclude that:

1. At very low nitrogen content (N/C < 0.4), nitrogen is bonded to sp^3-C forming CN single bonds and also occupies sites in aromatic rings.

2. Hydrogen is preferentially bonded to nitrogen. As N is added, the CH bonds disappear, increasing the sp^2 C fraction and the number of terminating NH bonds. This strongly suggests the use of hydrogen-free processes for an optimal deposition of carbon nitrides.

3. For higher N content, the originally sp^3-CN bonded matrix is mostly transformed into a polymeric configuration containing >C=N– structures.

The changes in the structural properties as nitrogen is incorporated depend upon the C–N bonding, which is highly complex [14]. EELS results show that nitrogen is mainly

sp^2 bonded to sp^3 C atoms, so nitrogen is threefold-coordinated with the other two electrons forming a lone pair. As the nitrogen content increases, the nitrogen atoms get closer and there can be a strong repulsion between nitrogen lone pairs. Some calculations suggest that N–N lone pair repulsion is a destabilising effect for the high density C_3N_4 structures [36]. Similarly, tight-binding molecular dynamics calculations [37] of N incorporation into C systems indicate that N favours C sp^2 and sp^1 bonding, with N developing CN double and triple bonds, resulting in an increase in the separation of neighbouring N atoms and therefore reduction in the lone pair interaction. Repulsion between adjacent lone pairs might be the driving force for the changes in the bonding configuration with increasing N percentage and might be one of the active mechanisms impeding the inclusion of high concentrations of N in CN deposits. This is not the case for Si_3N_4 or Ge_3N_4, where the large size of the Si or Ge atoms increases the N–N distance, so lone pair–lone pair repulsion is low.

Another prediction of the tight binding calculations [37] is a decrease in the film density with increasing N incorporation rates, as observed in our a-C:N:H films. This reduction in density has an important consequence, as it affects the resultant growth mechanisms. In a-C:H the incident ions promote dehydrogenation and formation of tetrahedral C bonds if they are able to densify the forming film by plastic deformation. However, in a low density or floppy film the subsurface implanted ions are accommodated without resistance, therefore, there is no driving force for the promotion of sp^3 bonds.

The main difference between these films and previous works [14, 38] is that our a-C:H films have a higher sp^3 content because of our high plasma density source. In the a-C:H films of other groups, that have a high sp^2 content, nitrogen often substitutes sp^2 C atoms, so no significant structural transition is observed.

5. Conclusions

Amorphous $C:N_x:H$ films ($0 \leq x < 0.7$) were deposited using a nitrogen/acetylene gas mixture in an ECWR source, which has previously been shown to produce highly tetrahedral amorphous hydrogenated carbon films. It was found that chemical sputtering limits the growth rate whereas the formation of molecular nitrogen within the film limits the nitrogen content. Nitrogen incorporation was also found to induce a change from a sp^3 hybridised C–N network to a polymeric >C=N–H structure.

Acknowledgements S. Rodil acknowledges financial support from CONACyT and ORS award scheme for a postgraduate scholarship. We thank N. Conway, V. Stolojan and D. N. Jayawardene for the EELS measurements and M. C. Polo for the XPS measurements. This project was fund by the UK Engineering and Physical Research Council.

References

[1] J. Robertson, Progr. Solid State Chem. **21**, 199 (1991); Diamond Relat. Mater. **2**, 984 (1993).
[2] Y. Catherine, in: Diamond and Diamond-Like Films, Vol. 266, NATO Advanced Study Institute, Ser. B, Ed. R. E. Clausing, Plenum Press, New York 1991 (p. 193).
[3] D. Ehrhardt, R. Kleber, A. Kruger, W. Dworschak, K. Jung, I. Muhling, F. Engelke, and H. Metz, Diamond Relat. Mater. **1**, 316 (1992).
[4] M. Weiler, S. Sattel, T. Giessen, K. Jung, and H. Ehrhardt, Phys. Rev. B **53**, 1594 (1996).
[5] Y. Lifshitz, S. R. Kasi, and J. Rabalais, Phys. Rev. Lett. **68**, 620 (1989).

[6] A. Liu and M. Cohen, Science **24**, 841 (1989); Phys. Rev. B **41**, 10727 (1990).
[7] D. F. Franceschini, F. L. Freire, and S. R. P. Silva, Appl. Phys. Lett. **68**, 2645 (1996).
[8] D. J. Johnson, Y. Chen, Y. He, and R. H. Prince, Diamond Relat. Mater. **6**, 1799 (1997).
[9] S. Muhl, A. Gaona-Cuoto, J. M. Mendez, S. Rodil, G. Gonzalez, A. Merkulov, and R. Asomoza, Thin Solid Films **308/309**, 228 (1997).
[10] N. A. Morrison, S. Muhl, S. E. Rodil, A. C. Ferrari, M. Nesládek, W. I. Milne, and J. Robertson, phys. stat. sol. (a) **172**, 79 (1999).
[11] M. Weiler, K. Lang, E. Li, and J. Robertson, Appl. Phys. Lett. **72**, 1314 (1998).
[12] Rusli and G. Amaratunga, Appl. Optics **34**, 7914 (1995).
[13] P. Hammer, M. A. Baker, C. Lenardi, and G. Lisser, Thin Solid Films **290/291**, 107 (1996).
[14] S. R. P. Silva, J. Robertson, G. A. J. Amaratunga, B. Rafferty, L. M. Brown, D. F. Franceschini, and G. Mariotto, J. Appl. Phys. **81**, 2626 (1997).
[15] Y. M. Ng, C. W. Ong, X. A. Zhao, and C. L. Choy, J. Vac. Sci. Technol. A **17**, 584 (1999).
[16] K. J. Boyd, D. Marton, S. S. Todorov, A. H. Al Bayati, J. Kulik, R. A. Zhur, and J. W. Rabalais, J. Vac. Sci. Technol. A **13**, 2110 (1995).
[17] N. Takada, K. Arai, S. Nitta, and S. Nonomura, Appl. Surf. Sci. **113/114**, 274 (1997).
[18] N. Hellgren, M. P. Johansson, E. Broitman, L. Hultman, and J. Sundgreen, Phys. Rev. B **59**, 5162 (1999).
[19] J. P. Biersack and G. L. Haggmark, Nucl. Instrum. and Methods **5**, 257 (1980).
[20] P. Hammer and W. Gissler, Diamond Relat. Mater. **5**, 1152 (1996).
[21] D. Marton, K. J. Boyd, and J. W. Rabalais, Internat. J. Mod. Phys. B **9**, 3527 (1995).
[22] J. Hartman, P. Siemroth, B. Schultrich, and B. Rauschenbach, J. Vac. Sci. Technol. A **15**, 2983 (1997).
[23] J. H. Kauffman, S. Metin, and D. D. Saperstein, Phys. Rev. B **39**, 13053 (1989).
[24] L. G. Jacobson, F. L. Freire, D. F. Franceschini, M. M. Lacerda, and G. Mariotto, J. Vac. Sci. Technol. A **17**, 545 (1999).
[25] C. Ronning, H. Feldermann, R. Merck, and H. Hofsass, Phys. Rev. B **58**, 2207 (1998).
[26] P. Hammer, N. M. Victoria, and F. Alvarez, J. Non-Cryst. Solids **227/230**, 645 (1998); J. Vac. Sci. Technol. A **16**, 2941 (1998).
[27] J. M. Ripalda, I. Montero, and L. Galan, Diamond Relat. Mater. **7**, 402 (1998).
[28] G. Beamson and D. Briggs, High Resolution XPS of Organic Polymers: The Scienta ESCA300 Database, Wiley & Sons, New York 1992.
[29] S. Grigull, W. Jacob, D. Henke, C. Spaeth, L. Summchen, and W. Siegle, J. Appl. Phys. **83**, 5185 (1998).
[30] C. Spaeth, M. Kuhn, F. Richter, U. Falke, M. Hietschold, R. Kilper, and U. Kreissig, Diamond Relat. Mater. **7**, 1727 (1998).
[31] S. Souto, M. Pickholz, M. C. dos Santos, and F. Alvarez, Phys. Rev. B **57**, 2536 (1998).
[32] S. D. Berger, D. R. Mackenzie, and P. J. Martin, Phil. Mag. Lett. **57**, 285 (1988).
[33] L. Wan and R. F. Egerton, Thin Solid Films **279**, 4 (1996).
[34] R. F. Egerton, Electron Energy-Loss Spectroscopy in the Electron Microscope, 2nd ed., Plenum Press, New York 1996.
[35] A. Libassi, A. C. Ferrari, N. A. Morrison, V. Stolojan, B. K. Tanner, J. Robertson, and L. M. Brown, unpublished.
[36] T. Hughbanks and Y. Tian, Solid State Commun. **96**, 321 (1995).
[37] F. Weich, J. Widany, and Th. Frauenheim, Phys. Rev. Lett. **78**, 917, 3326 (1997).
[38] J. Schwan, V. Batori, S. Ulrich, H. Ehrhardt, and S. R. P. Silva, J. Appl. Phys. **84**, 2071 (1998).